

A Model of Gastric Electrical Activity in Health and Disease

Babajide O. Familoni, Thomas L. Abell, and Kenneth L. Bowes

Abstract—The idea of diagnosing gastric dysfunction from noninvasive measurements of gastric electrical activity (GEA) is intuitively appealing, but the predictive accuracy of the cutaneous signal, especially that of its amplitude, is still in question. Mathematical modeling provides a means of investigating, analyzing, and predicting GEA measured percutaneously. In this study, a model of GEA applicable both in health and disease was developed and simulated for a cylindrical body surface. Body-surface maps of the simulated electrogastrogram (EGG) were generated at a 20 by 20 array of sites on the model's surface, and the accuracy of the percutaneous method in detecting simulated gastric electrical abnormalities was determined. The relationship between the amplitude of the simulated surface EGG and the velocity of propagation of the myogenic activity was also investigated. This was compared to a similar investigation of the fluctuations in the amplitude of the surface EGG with the velocity of propagation of the serosal activity measured in humans. The diagnostic accuracy of the measured cutaneous EGG in humans was also determined. The results obtained from the mathematical model show that the amplitude of the electrogastrogram increases with the propagation velocity of GEA. Similar results were obtained from the experimental measurements. The amplitude of the simulated and measured cutaneous signal correlated well ($p < 0.05$) with the phase shift of the simulated and measured activities, (-0.85 , -0.54), respectively. Serosal normal activity, tachygastric, and uncoupling were detected 67%, 90%, and 0% of the time, respectively, at the cutaneous electrode in humans. In simulations, normal activity and tachygastric were accurately detected at all 400 sites on the surface. Uncoupling simulated with 50% of the myogenic sources "diseased" was detected at only 20 of the 400 sites. The results confirm that the amplitude of the cutaneous signal is a function of the velocity of propagation of the myogenic signal. It also confirms that while GEA in health may be accurately predicted from percutaneous recordings, frequency and phase/coupling abnormalities are poorly detected from single-channel electrogastrograms. This suggests the use of multiple-channel surface recordings in clinical electrogastrography.

I. INTRODUCTION

THE NATURE of gastric electrical activity (GEA) in health is fairly well understood. In man, it consists of recurrent regular depolarizations (slow waves or electrical control activity—ECA) at 2.5 to 4 cycles per minute (cycles/min), and intermittent high-frequency oscillations (spikes or electrical response activity—ERA) that appear only in association with contractions. The oscillations commence at a pacemaker

Manuscript received November 1, 1993; revised February 22, 1995. This work was supported in part by Grant 1R15 DK 42662-01A2 from the National Institute of Diabetes and Digestive and Kidney Diseases.

B. O. Familoni is with the Department of Electrical Engineering, The University of Memphis, Memphis, TN 38152 USA.

T. L. Abell is with the Division of Gastroenterology, The University of Tennessee, Memphis, TN 38163 USA.

K. L. Bowes is with the Department of Surgery, University of Alberta Hospital, Edmonton, Alberta, Canada T6G 2B7.

IEEE Log Number 9411751.

site high up in the corpus and propagate aborally to terminate at the distal antrum. The velocity of propagation and the signal amplitude increase as the pylorus is approached. ECA are the ultimate determinant of the frequency and direction of propagation of phasic contractions, which are responsible for mixing and transporting gastric content [1]–[3]. Therefore, when gastric motility disorders occur, they are sometimes manifested as gastric electrical abnormalities. Since surface electrodes can be used to record the electrical activity [4]–[8], the concept of cutaneous electrodes diagnosing abnormalities in gastric electrical activity has great appeal. Their use in the clinical diagnosis of gastric motor dysfunction has already been advocated and demonstrated [9]–[16]. On the other hand, some studies have shown that the detection of gastric electrical abnormalities from the amplitude, phase, and frequency parameters of percutaneous recordings is problematic [17], [18].

Definite abnormalities in GEA have been described in only a few conditions with nonimplanted electrodes. In all such recordings, a good recording may not be obtained for part of the recording duration. The abnormalities described are usually present only a portion of the recording time and the incidence of noisy records are high. These abnormalities in ECA activity have been described utilizing the noninvasive technique in patients with unexplained nausea and vomiting [10], [11], anorexia nervosa [12], gastroparesis [13], [14], pregnancy-related nausea [15], and motion/space motion sickness [16]. Although comparing groups of patients with the same technique, as done in these studies, lends credence to the existence of an abnormality in a particular group, recent evidence has shown that the accuracy of transcutaneous electrogastrograms (EGG) in diagnosing an abnormality in a single patient is poor [17]. Moreover, the diagnostic usefulness of its amplitude before and after a meal have been shown to be misleading [18]. The clinical usefulness of this tool remains limited by lack of understanding of several features of the recorded EGG.

Empirical methods can take electrogastrography only so far. If EGG is to achieve its potential as a clinical diagnostic tool, a better understanding of the relationship between the gastric activities (especially the abnormalities) and what is recorded at the skin is required. Rigorous analytical methods to standardize and improve the diagnostic accuracy of EGG's may help achieve this goal. Such an understanding may be approached from a mathematical model and computer simulation point of view, as a starting point. Experimental validation of such modeling may then follow.

A few models of GEA have been reported [19]–[23]. The models are often based on the concept of the forward problem in volume conductors, which have been so successful in

electrocardiography and electrical conduction studies in active nerve fibers [24]–[26]. These models simulated GEA in health. While studies of EGG in health are educative, the diagnostic potential of the method is evidenced by its ability to predict GEA in the diseased state. In the present study, a model of the forward problem in electrogastrigraphy was developed and simulated for health or disease. The model was employed to explore and resolve the dilemma on the diagnostic usefulness of the amplitude of cutaneous GEA. The simulated results were also compared with simultaneous measurements of cutaneous and serosal EGG's in humans.

II. MATHEMATICAL SIMULATION

In an earlier study, a mathematical model of the electrically active antral part of the stomach based on a solution of the forward problem in a homogeneous conducting medium was reported [19]. In that model, the sources within the volume were modeled as dipole sources. The resulting Poisson's equation describing the time dependent potential ϕ as a function of vector location \underline{r} for a given source vector \underline{P} is

$$\nabla^2 \phi(\underline{r}, t) = \underline{P} \quad (1)$$

subject to the boundary conditions

- 1) $\phi(t)$ is finite within a homogeneous volume conductor bounded by a cylindrical surface, and
- 2) $\left[\frac{d\phi}{dn} \right]_s = 0$, i.e., Neumann's boundary condition holds for the normal vector \underline{n} at the conductor-air interface, s .

Unlike cardiac muscle, gastrointestinal muscles do not function as a syncytium in which the electrical activity is controlled from a single focused pacemaker site. Instead, the different oscillating sites generate their own activity and merely exhibit coupling with their nearest neighbors in the circular and longitudinal directions. This fact makes it particularly convenient to model small regions as independent oscillating sites that are coupled to their nearest neighbors [19]–[23]. The linear array of signal sources were located in the cylinder at approximately the same region as the gastric antrum in man, (r_0, θ_0, z_0) . Since the system is quasi-stationary, the source signals were sampled in time and space. The myogenic sources were represented as a spatial array of 22 coupled single dipoles $f(k, t)$, $k = 1, 2, \dots, 22$, spaced 0.5 cm apart, and each resolved into its r, θ , and z components (see Appendix). Such a linear array ensures propagation in the longitudinal direction. This does not imply a lack of organized propagation in the circular direction. On the contrary, perfect coupling in the circular direction is implied. Previous researchers have already shown that coupling in the circular direction is much tighter than in the longitudinal direction [1], [22], [23]. Sarna estimated coupling in the circular and longitudinal directions in the antrum in dogs to be about 0.22 and 0.57, respectively [23]. In this study, for the sake of simplicity, instantaneous spread of electrical activity is assumed in the circular direction and propagation in the longitudinal direction is effected as discussed later.

The source vector \underline{P} is expressed as

$$\begin{bmatrix} P_r \\ P_\theta \\ P_z \end{bmatrix} = \begin{bmatrix} f_r(k, t) \\ f_\theta(k, t) \\ f_z(k, t) \end{bmatrix}$$

and the resulting cutaneous potentials calculated as a superposition of the corresponding sampled potentials at the surface. The time dependent potential $\phi(\underline{r}, t)$ at a vector location \underline{r} on a finite length cylinder of radius A , was assumed to represent the potential generated in the body.

This paper presents a model of GEA applicable in health and disease. The source function $f(k, t)$ of the individual sources varies as a function of time t , in much the same manner as the measured intracellular potentials in the gastric musculature in health. These source functions may be described as

$$f(k, t) = a_k \cdot F(\omega_k t + \beta_k) \quad (2)$$

where ω_k is the basal rhythm (in rads/s) and β_k is the phase shift (in radians) of the k th source signal. $F(\cdot)$ represents an approximation of the intracellular source function in man [19] and a_k is the amplitude of the antral signal at the different oscillating sites as the pylorus is approached. In order to address the gradual increase in amplitude of GEA in the distal direction in humans, the amplitude of the k th source, a_k , was expressed as a function of its position along the greater curvature as

$$a_k = \begin{cases} 0.177e^{0.124k}, & 1 \leq k < 14 \\ 1, & 14 \leq k \leq 22. \end{cases} \quad (3)$$

This amplitude function for the oscillating sites was derived by fitting an exponential function to experimental measurements of GEA at eight sites in the human stomach. GEA was measured with bipolar stainless steel electrodes implanted serosally at 1-cm intervals along the greater curvature. The electrode positions and signal amplitudes were then fitted to an exponential function in a least square sense to obtain the approximation in (3).

In health, GEA throughout the antrum is electrically coupled. This coordinated activity is achieved because the velocity of propagation of the activity is dependent on the length of the antrum, such that peristaltic contractile activity at the terminal antrum is one cycle behind that at the proximal antrum, i.e., $\beta_{22} = \beta_1 + 2\pi$. This implies that an activity wavefront reaches the terminal antrum just as the next wave begins in the proximal stomach. The net effect of this is that a single ring of peristaltic contraction terminates at the pylorus just as a new one begins in the proximal stomach. This phenomenon has been described in cinefluoroscopy studies by Stern and Koch [27]. Also $\omega_k = \omega_0$, for all k . If the average phase shift over the entire antrum is assumed to be β_0 (rads/cm), to ensure phase-locking and uniform propagation in an aborad direction, the phase shift at the k th source must be

$$\beta_k = (k - 1) \cdot \beta_0. \quad (4)$$

The mean velocity of propagation of GEA in the antrum, V_0 , is a function of the antral length, the average phase difference, β_0 , and the period of the ECA T . Therefore, the average phase difference in (4) above is $\frac{360^\circ}{T \cdot V_0}$, i.e.,

$$\beta_0 = \frac{360^\circ}{0.5 \cdot q \cdot T \cdot F_s} \quad (5)$$

where 0.5 cm is the spatial sampling distance, $T_s = 1/F_s$ is the temporal sampling period, and q is a constant that

permits one to change the average velocity of propagation. The average phase delay, β_0 , reported in the longitudinal direction in the human stomach is $45^\circ/\text{cm}$ [8]. Coupling in the circular direction is tighter and the phase shift much smaller [22], [23]. As explained earlier, this model assumes that spread in the circular direction is instantaneous.

As a consequence of temporal sampling at a rate F_s (6 Hz) and spatial sampling at 2 sources/cm, the surface potential at the sample instance $t = lT_s$ can be computed as contributions from every oscillating source from $k = 1$ through 22 as

$$\phi(\mathbf{r}, lt_s) = \sum_{k=1}^{22} [\phi_r(i_k T_s) + \phi_\theta(i_k T_s) + \phi_z(i_k T_s)] \quad (6)$$

where i_k is given by $i_k = lT_s + (L-k) \cdot m$, l and m are integers. The contribution of the k th oscillating source to the r , z , and θ components of the potential ϕ at $t = lT_s$, ($\phi_r(\cdot)$, $\phi_\theta(\cdot)$, and $\phi_z(\cdot)$) are as developed in the Appendix.

The source function and phase shifts represented by (2) through (6) were modeled to mimic the intracellular activity: 1) in health at different velocities of propagation, 2) during frequency abnormalities, and 3) phase abnormalities. From these, the simulated surface EGG's were computed on a VAX mainframe computer. The distribution of the activity over the surface of the cylinder (representing the torso) was investigated by partitioning the anterior surface ($r = A, 0^\circ \leq \theta \leq 180^\circ, 0 \leq z \leq h$) into a 20 by 20 grid, with the corner of every grid being a potential electrode location. The surface potential $\phi(\mathbf{r}, t)$ at the vector location \mathbf{r} on the surface was then expressed as a matrix

$$\phi(\mathbf{r}, t) = \phi_{ij}(t), \quad i, j = 1, 2, \dots, 20. \quad (7)$$

$\phi_{ij}(t)$ was simulated for approximately two waveform cycles (41 s) and its spectrum $s_{ij}(\omega)$ computed by way of the fast Fourier transform (FFT).

In clinical electrogastronomy, one is often interested in determining if the gastric signal is present in the "normal window" all the time, and if not, what type of abnormality is indicated by the recording. Because of the poor quality of the signal, spectrum analysis is frequently employed in making these determinations. A similar strategy was employed to quantify the simulated signal.

Let the "normal window" be defined as $\omega_0 - \omega_1 \leq \text{freq.} \leq \omega_0 + \omega_2$ ($2.5 \text{ cycles/min} \leq \text{freq.} \leq 4 \text{ cycles/min}$), the signal strength in this window p_n , and a Signal-to-Noise ratio (SNR) number, Q_{ij} . This number is a measure of the relative strength of the normal signal peak p_n compared with the noise and the abnormal signal peaks, i.e.,

$$Q_{ij} = \left[\frac{p_n}{p_t - p_n} \right]_{ij}; \quad i, j = 1, 2, \dots, 20 \quad (8)$$

where $p_t = (s_{ij} \cdot s_{ij}^*)$ is a measure of the total power in the whole spectrum from dc to 3 Hz, and the normal signal peak is given by $p_n = |s_{ij} \cdot s_{ij}^*|_{\text{normal window}}$; "*" indicates complex conjugate.

A. Simulated Surface EGG as a Function of the Velocity of Propagation

The phase shift/cm was varied from -70° to $+70^\circ$ by adjusting the quantity q in (5) as $-12 \leq q \leq 12$ and the surface EGG computed. The corresponding energy in the signal at the conductor air interface was calculated as

$$E = \int_0^T \phi(r, t) \cdot \phi^*(r, t) dt \quad (9)$$

by numerical integration. Solutions were generated on a VAX mainframe computer for the different values of phase lag in the source signal embedded in the volume conductor.

B. Simulation of Abnormalities

The nature of the abnormalities recorded in implanted electrode studies are well known and fall into two main categories [17], [28]–[31]: 1) abnormalities involving shift in frequency from ω_0 to a value outside the normal range, and 2) electrical uncoupling of adjacent oscillating sites. Often, the frequency shift is upwards to about 6–8 cycles/min; this is termed tachygastric. Uncoupling may result from one of two mechanisms. The first is a phase-unlocking of the sources, i.e., β_k becomes random while the frequency of the signal ω_k at each oscillating source remains ω_0 . A second mechanism is indicated when each oscillating source or group of sources oscillate at its own unique frequency ω_k . In actual patient studies, only two or three different frequencies are identifiable. The tissue masses merely group into two or three locally coupled oscillating regions at frequencies different from those of the nearest neighbors [17]. In this study, we have simulated these abnormalities. The source function in (2) has two parameters that may be varied for each source k , i.e., frequency of oscillation ω_k and the phase β_k .

1) *Frequency Uncoupling Abnormality*: The oscillating sources were divided into a normal ($k = 1, \dots, k_1$) and an abnormal or "diseased" ($k = k_1 + 1, \dots, 22$) group, whose relative population may be varied by simply varying the number k_1 . Normal sources represent tissues oscillating at the normal gastric frequency ω_0 , while diseased sources oscillate at a different nonharmonic frequency ω_t ($= 6.8 \text{ cycles/min}$). This effected frequency uncoupling of the "healthy" segment from the "diseased" segment. When the relative population of the abnormal sources become 100%, the calculated potentials represent those for simulated tachygastric. It is important to make the frequency representing tachygastric a noninteger multiple of ω_0 . This avoids the possibility of detecting harmonics of the fundamental and the introduced abnormality as one and the same.

2) *Phase Shift Abnormality*: Phase uncoupling was simulated by letting all the sources oscillate at the same frequency ω_0 , with their phase β_k generated by a random number generator. This effects a phase-unlocking of adjacent oscillating sites. A function $g(k)$ representing the spatial rate of change of the phase β_k was defined; $g(k)$ is inversely proportional to the propagation velocity. In the intact human stomach, the phase gradient $g(x) = \frac{d\beta}{dx}$, where x is the displacement along the greater curvature. In this sampled model, $x = 0.5 \text{ k}$, $k =$

0, 1, 2... and $g(k) = \beta_k - \beta_{k-1}$. To simulate phase uncoupling, $g(k)$ was defined as

$$g(k) = \beta_0(1 + \text{Random}(n)). \quad (10)$$

In order to introduce graduated levels of abnormality, the range of the random number generator was made adjustable. By changing this range or wobble factor, one may simulate a whole spectrum of coupling abnormalities from a very mild wobble in phase shift, i.e., $\frac{g(k)}{\beta_0} = 1 + \xi$, $\xi \ll 1$, to gross antral uncoupling, i.e., $\frac{g(k)}{\beta_0} = 2$.

III. MATERIALS AND METHODS

For comparison, simultaneous measurements of GEA were made from two pairs of cutaneous and three pairs of serosal electrodes in six patients. The study was approved by the ethics committee of the University of Alberta Hospitals and informed written consent was obtained from each subject before the procedure. The recordings were made in patients undergoing laparotomy for fundoplication, cholecystectomy, or bowel resection. Three pairs of stainless steel wire electrodes, 0.254 mm in diameter, were implanted subserosally into the anterior surface of the antral wall, between 1.5 cm and 10.5 cm from the pylorus. The Teflon-coated connecting wires were brought out through the surgical drain. EGG was also recorded percutaneously from four ordinary Hewlett-Packard electrocardiography electrodes (type 14445C) located on the skin in the epigastric region to form two bipolar channels. Each pair was aligned with the antral axis as previously described [4], [17] or as close to it as the surgical wounds permitted.

The serosal channels were band-limited to frequencies between 0.017 Hz (1 cycles/min) and 30 Hz (1800 cycles/min) on a Sensomedic dynograph recorder, while the cutaneous channels were limited to frequencies between 0.017 Hz (1 cycles/min) and 0.08 Hz (4.8 cycles/min). The roll-off on these filters attenuates respiratory and cardiac artifacts while still passing tachygastria and signals up to the third harmonic frequency of normal GEA. The signals at the dynograph amplifier outputs were sampled at a rate of 2 Hz and stored on an IBM compatible computer via a LabMaster 200009 12-b, eight-channel A-to-D converter (Scientific Solutions, Solon, OH). Recording was initiated immediately following surgery and continued for 96 h.

All channels were subjected to both visual and computer analysis. The recorded signals were visually inspected for regularity in the period of the activity, and for presence of abnormalities. The time length of segments showing abnormalities on the serosal recording was noted and compared with a similar evaluation of the cutaneous recording. Those sections of the record in which increases occurred in the amplitude of the transcutaneous signal for six or more ECA cycles were selected by visual inspection. If such increases occurred within one hour of feeding, they were excluded from further analysis. GEA recorded from the serosal electrodes in those sections chosen were visually inspected for spontaneous changes in amplitude and then cross-correlated over successive 128-s intervals to yield the average phase lag for the intervals [3] (Fig. 1). Sequential spectral analyses over successive 128-s

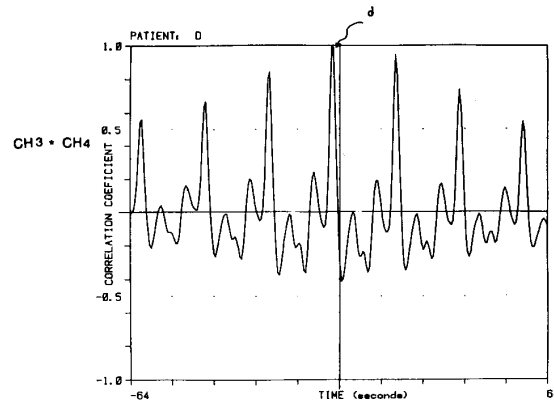


Fig. 1. Cross-correlation of two serosal records of gastric electrical activity as a function of time. The common period of the activities is 20.6 s. The phase shift (degrees) from channel 3 to channel 4 in this figure is determined as $\frac{d \cdot 360^\circ}{20.6} = 45.7^\circ$.

intervals were also performed on the signals in the same segment by employing FFT with a hamming window. The relative power in the transcutaneous signal was approximated by the height of the fundamental and the first harmonic in the power spectrum analysis, while that of the serosal signal was defined as the sum of the amplitude of the fundamental and all its harmonics (Freq $\leq 60/\text{min}$). Descriptive statistics were computed on a VAX mainframe computer, and Pearson cross-correlation analysis was employed to examine the relationship between the relative power in the transcutaneous signal and the phase shifts of the serosal activity. The relative power averaged over both cutaneous channels was correlated with the average of the phase shift between adjacent serosal electrodes. Follow-up analyses were performed with the significance level set at 0.05.

Periods of nursing care or patient movement as marked on the recording paper by the nursing staff were excluded in the analysis. The implanted electrodes were removed with the drain when the latter was no longer needed -72 to 120 h after its insertion.

IV. RESULTS

A. Simulation Study

The time course of change of the surface potentials calculated in the healthy model was similar to that measured in health in humans. This normal activity was confirmed by the power spectrum over most of the anterior surface. Fig. 2(a) shows a three-dimensional (3-D) plot of the normal signal strength p_n over the anterior surface of the torso. The strongest signal peak p_n occurred in an anterior patch of the surface defined by $60^\circ < \theta < 135^\circ$ and $0.2 \text{ m} < z < 0.45 \text{ m}$. This area is readily identifiable on the surface contour map in Fig. 3(a) as the area with the dense population of contour lines. At other locations, the signal strength of the normal component of the simulated EGG falls off and the waveforms degraded considerably. Power spectrum analysis of such waveforms still revealed a recognizable peak in the "normal window."

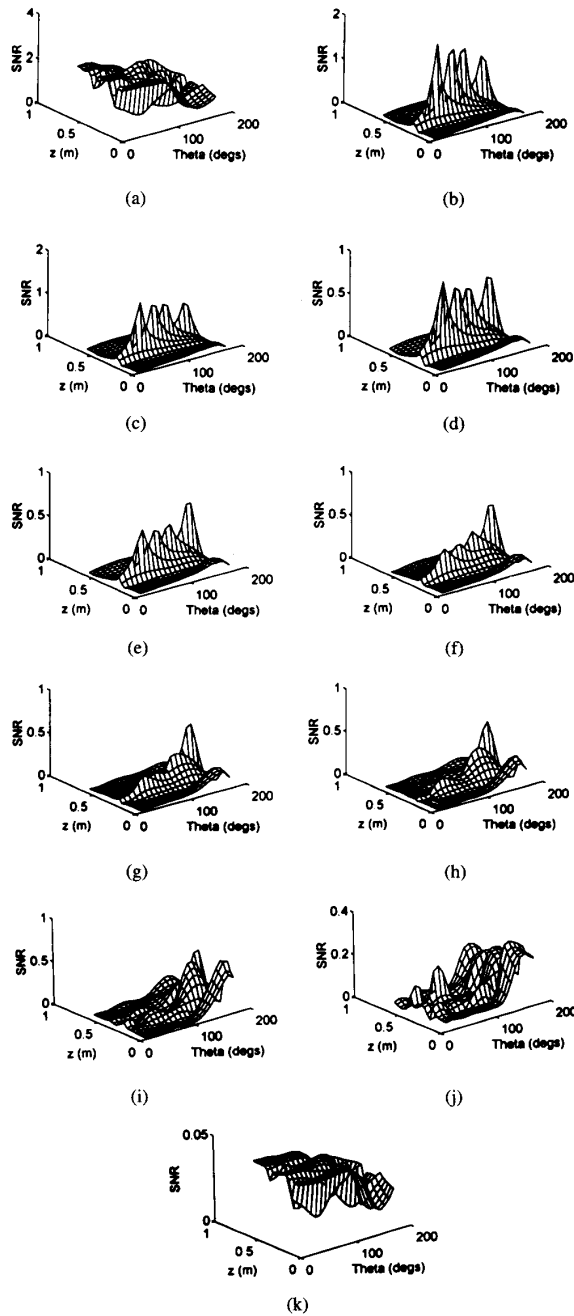


Fig. 2. Three-dimensional mapping of the signal to noise ratio (SNR) of the simulated surface electrogastragram. In (a), the whole antrum exhibits a single frequency of 3 cycles/min and is therefore normal. In (b)–(k), similar plots are shown for the diseased model with the stomach into a “healthy” and “diseased” segment, exhibiting two frequencies at 3 and 6.8 cycles/min, respectively. In (b), abnormality occurred in 9.5% of the sources and in increasing steps of 9.5% of the sources, up to 95% in (k).

Introduction of frequency abnormality reduced the amplitude of the normal signal detected on the surface and its strength p_n . The area over which the normal component was detectable also shrunk (Figs. 2(b)–(k) and 3(b)–(k)). Phase uncoupling had the greatest effect on the strength of the

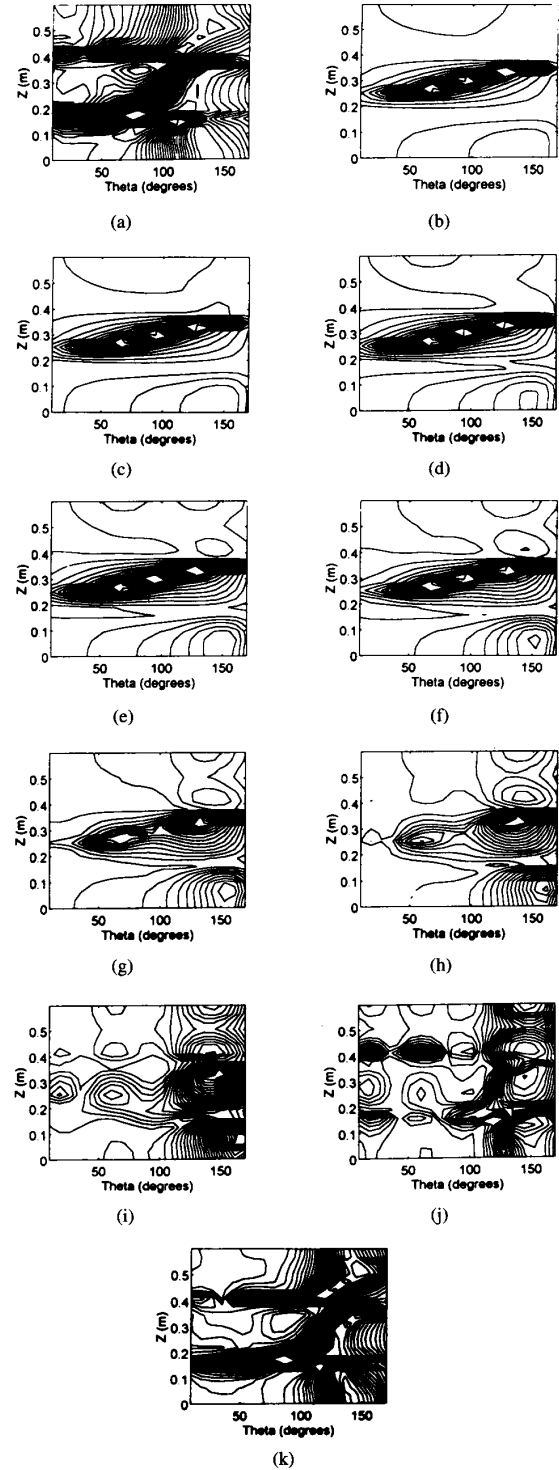


Fig. 3. Contour maps of the signal-to-noise ratio of the simulated surface electrogastragram. In (a), the whole antrum exhibits a single frequency of 3 cycles/min and is therefore normal. In (b)–(k), similar plots are shown for the diseased model with the stomach into a “healthy” and “diseased” segment, exhibiting two frequencies at 3 and 6.8 cycles/min, respectively. In (b), abnormality occurred in 9.5% of the sources and in increasing steps of 9.5% of the sources, up to 95% in (k).

TABLE I
RELATIVE STRENGTH OF THE NORMAL COMPONENT OF SIMULATED GASTRIC ELECTRICAL ACTIVITY CALCULATED AT THE SURFACE OF THE MODEL

State of Model	Mean of Maximum $p_r \pm$ Standard Deviation (Arbitrary Units)
Normal Activity	2.056 ± 0.48
Frequency Abnormality	0.506 ± 0.21
Phase Abnormality	0.336 ± 0.56

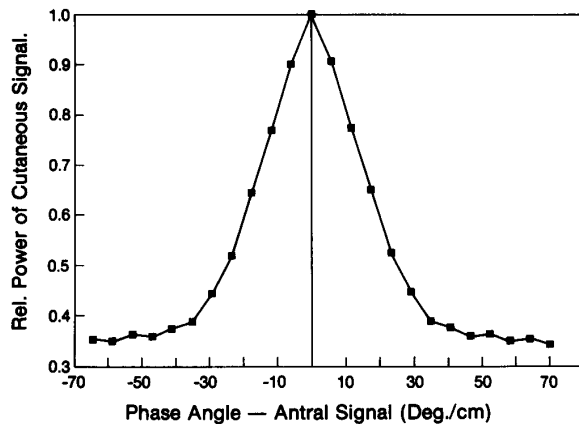


Fig. 4. Relative power of simulated cutaneous electrogastrogram plotted as a function of the phase shift of the serosal activity for forward and retrograde propagation. A zero phase shift implies that the activities at adjacent sites appear simultaneously.

surface signal. With even small values of the wobble factor, the strongest signal's region shrunk appreciably, the mean magnitude reduced as in Table I, and the simulated surface signal became very noisy.

Changes in the velocity of propagation of the simulated antral activity did not change the shape or frequency of the simulated EGG at the surface. The relative power in the simulated surface EGG as given by (9) varied inversely with the phase angle of the antral GEA during forward and retrograde propagation (Fig. 4). The correlation between power in the simulated cutaneous signal and the phase shift of the simulated antral signal was -0.85 , $p < 0.05$.

B. Human Study

A total of 491.9 h of recording were obtained. Of this, 7.3 h of all recordings were contaminated with noise from patient motion and nursing care. Data analysis was restricted to the remaining 484.6 h. The recorded GEA was normal in 76.84% of the portion analyzed. During normal activity, statistically similar frequencies (mean \pm standard deviation) were observed on both the serosal (2.91 ± 0.48 cycles/min or 0.049 ± 0.01 Hz) and cutaneous tracings (2.86 ± 0.47 cycles/min or 0.048 ± 0.01 Hz); ($p < 0.05$). These frequencies are similar considering that the frequency resolution of the FFT procedure in this application is 0.47 cycles/min. Average amplitudes of the serosal and cutaneous signals over the entire record were 0.363 ± 0.29 mV and 0.051 ± 0.02 mV, respectively.

TABLE II
BREAKDOWN OF SEGMENTS WITH TRANSIENT FLUCTUATIONS IN THE AMPLITUDE OF PERCUTANEOUS GASTRIC ELECTRICAL ACTIVITY RECORDED IN SIX POSTOPERATIVE PATIENTS

Patient N°	# of amplitude transients analyzed	Mean duration \pm standard deviation (min.)	Correlation with serosal phase shift
1	7	12.33 ± 6.7	-0.6997
2	2	8.66 ± 2.5	-0.1928@
3	0	-	-
4	3	10.13 ± 6.1	-0.7716
5	2	7.82 ± 3.5	-0.5998
6	5	22.03 ± 18.5	-0.8106

Nineteen episodes of spontaneous increases in the amplitude of the cutaneous EGG recorded in five of the six patients were analyzed. These spontaneous increases in amplitude of the cutaneous EGG were not accompanied by comparable changes in the amplitude of the serosal signal or any abnormality (Fig. 5). The frequency of the activity remained normal and signals recorded at all sites in the antrum were coupled (Fig. 6). The relative power of the cutaneous signal exhibited an inverse relationship with the phase angle with a correlation coefficient of -0.54 , $p < 0.05$ (Fig. 7 and Table II).

Abnormalities in GEA recorded at the serosa appeared in five patients shortly after the post-recovery room period. The abnormalities lasted up to 10.75 ± 4.61 h postoperatively in four, and persisted until the implanted electrodes were removed in the fifth, (101 h later). These abnormalities included 131 episodes of tachygastric with an average duration of 45.9 ± 74.3 min, and nine episodes of uncoupled activity with an average duration of 217.3 ± 92.4 min. Ninety-one percent of the time existing tachygastric at the serosa was recognizable at the percutaneous record. Percutaneous EGG's did not recognize uncoupled gastric electrical events (Fig. 8).

V. DISCUSSION AND CONCLUSION

Important parameters of GEA that may be measured and employed in disease diagnosis include its rhythm or regularity, period or frequency, amplitude or power, and coupling or coordination. If the activity in the stomach is coupled, the rhythm of the percutaneous signal tracks that of the serosal activity and recognition is elementary. The normal frequency range of occurrence of GEA is well known (2–3.6 cycles/min) and departures from this are generally accepted as an indication of disease [9], [32]. Detection of such frequency abnormalities from percutaneous recordings is reliable [17].

Previous studies have asserted the physiological importance and diagnostic potential of the amplitude or power of percutaneous EGG [32]–[36]. This amplitude of the transcutaneous signal is influenced by a number of parameters including the electrode-skin interface impedance, the conductivity of the torso, the thickness of the tissue over the stomach wall, and the strength of the antral signal. According to Smout *et al.*, the strength of the antral signal is, in turn, affected by the presence of ERA [32], [33]. This mix of factors complicates the use of EGG amplitude as a diagnostic parameter. One

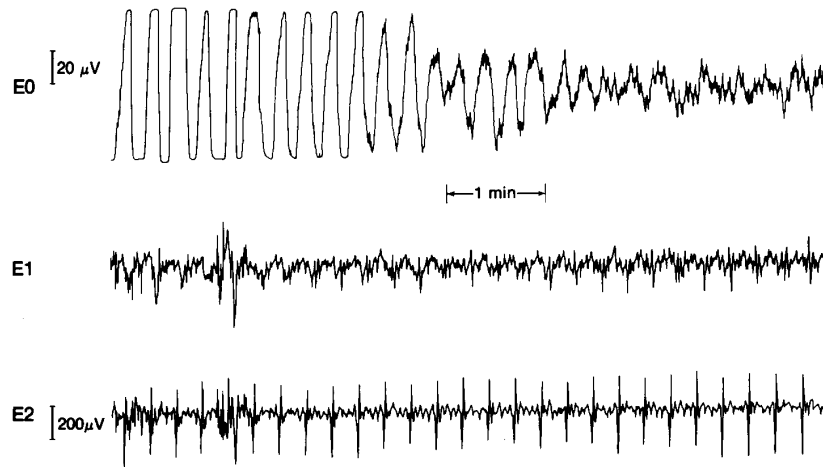


Fig. 5. Gastric electrical activity recorded by serosal ($E1, E2$) and cutaneous ($E0$) electrodes in a postoperative patient. The amplitude of the percutaneous record ($E0$) fluctuates spontaneously.

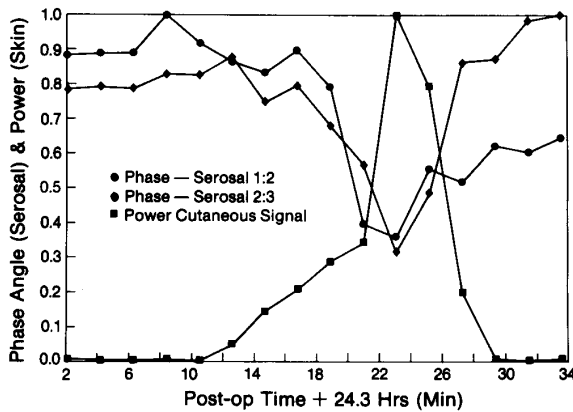


Fig. 6. Normalized power of the percutaneous signal and normalized phase shift of the serosal signal in a postoperative patient plotted as a function of time during a 34-min episode of spontaneous fluctuations in the amplitude of the percutaneous signal. The phase shift between $E1$ and $E2$ tracks that between $E2$ and $E3$ indicating phase locking.

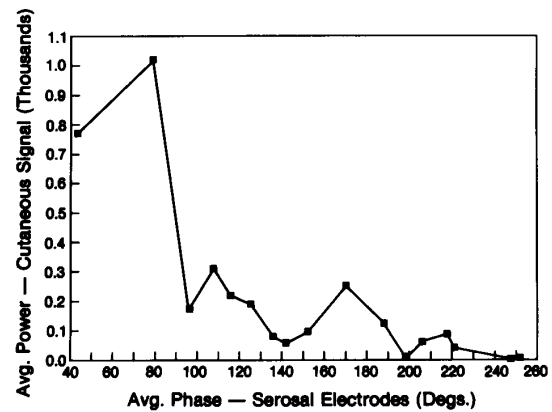


Fig. 7. Relative power of the cutaneous signal versus phase angle of the serosal record averaged over six postoperative patients. Note the similarity between Fig. 4 obtained from the mathematical model and this experimental result.

diagnostic application of EGG amplitude that has been widely reported as useful involves percutaneously measuring the EGG before and after the application of a stimulus such as food [27], [32]–[36]. In such “before and after” tests, diagnosis is based on the comparative amplitude of the cutaneous EGG before and after the test meal. One study has suggested that any amplitude differences may be due more to mechanical displacement and distention rather than physiological reasons [18]. By inflating intragastric balloons in anesthetized dogs pretreated with atropine and glucagon, Mintchev *et al.* showed that the amplitude of the surface EGG correlated with the displacement of the stomach wall, but not with contractions or the amplitude of serosal GEA. This calls into question the clinical relevance of the relative amplitude of EGG’s in fasted and fed studies and ordinarily would render this parameter of little clinical importance. Without refuting the effect of intragastric volume, our study reasserts the physiological relevance of the amplitude of the percutaneous EGG.

The mathematical model presented in this study showed that the amplitude and the power of the simulated cutaneous signal correlated with the velocity of propagation of the antral activity. These results were confirmed by simultaneous cutaneous and serosal measurements in postoperative patients. Therefore, if one were to separate the distention and propagation components, the amplitude of cutaneous EGG would be an indication of the velocity of propagation. This suggests the substitution of other stimuli such as pharmaceutical agents that enhance motility in the evaluation of “before and after” cutaneous EGG’s. However, before such studies can be meaningful, systematic studies examining the relationship between transients in the amplitude of percutaneous EGG and serosal phase shifts are warranted.

Electrical coupling is another important parameter of GEA. This coupling is evidenced by the coordination of its phase shift and its spatial differential. The actual phase of the intracellular activity in the healthy human stomach, $\beta(x)$, is a continuous function of the spatial variable x . Equations (4)

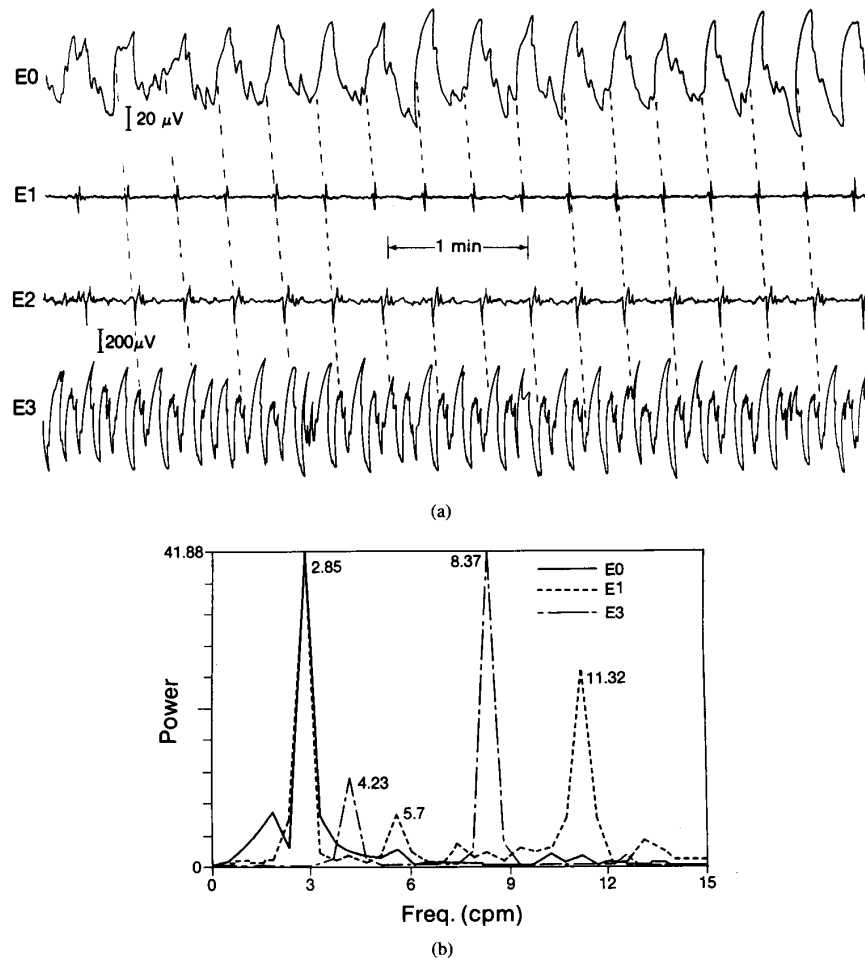


Fig. 8. (a) Uncoupled gastric electrical control activity recorded in a postoperative patient with implanted serosal electrodes $E1$, $E2$, and $E3$ in the antrum and cutaneous electrode $E0$ on the epigastric region. (b) Power spectrum of the record in (a). The percutaneous and proximal antral activities appear normal at a fundamental frequency of 2.85 cycles/min with harmonics at 5.7 and 11.32 cycles/min. The frequency of the activity at the most distal serosal site, $E3$, at 4.23 cycles/min is roughly 1.5 times that of the signals on the more proximal serosal electrodes, $E1$ and $E2$ and the cutaneous electrode, $E0$.

and (10) represent a discrete space model of the same. In the healthy human stomach, the electrical activity meets the following conditions:

- 1) $\beta(x)$ is continuous in the spatial variable x . Specifically, it is required that $\frac{d\beta}{dx} = g(x) > 0$, for all x .
- 2) $g(x)$ is continuous in space.

Condition 1) ensures net aboral propagation of the electrical activity, while the more stringent second condition ensures that the propagating activity is coupled. These two conditions, plus the limits imposed on $g(x)$ by the length of the antrum and mean antral propagation velocity, define coupled GEA in health. From actual measurements in man, Familoni *et al.* reported average values of $g(k)$ as $70^\circ/\text{cm}$ high up in the corpus and $25^\circ/\text{cm}$ in the terminal antrum [8]. Thus, the activity propagates aborally, accelerating as the pylorus is approached. As previously discussed, the continuous spatial variable in the actual system is represented in the model by a sampled variable engendered in the 22 discrete sources. Conditions 1) and 2) above still apply to the model if difference equation

equivalents are substituted. In condition 1) above, $g(k) = \beta_0$ is held constant in the simulation of the normal activity for ease of computation.

To simulate phase uncoupling, we allow $g(k)$ to be positive, but random. This ensures forward propagation but not coupling. This implies that local retrograde propagation may occur, but there is a net propagation toward the antrum. This, for example, may represent various kinds of delayed gastric emptying. We were not able to detect phase uncoupling from recorded or simulated EGG.

In theory, one should be able to diagnose frequency-uncoupled GEA from a single channel of percutaneous EGG. This is because every component of the uncoupled antral activity is represented in the surface recording. Hence, spectrum analysis should display these constituent frequencies. In practice, frequency spectrum analysis is not discriminating enough to separate elements of pseudowhite noise and physiological interferences from representations of small errant oscillating regions (diseased sources) in the stomach.

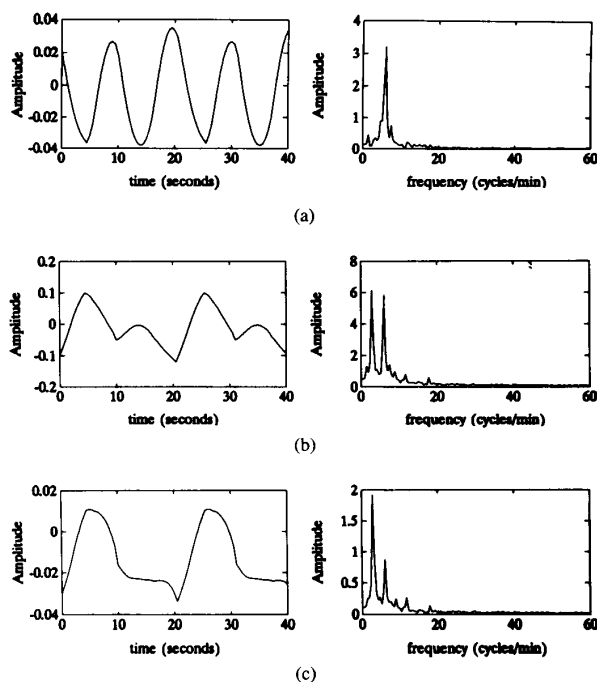


Fig. 9. Simulated surface electrogastragrams and their power spectra at different locations for the same frequency abnormality ($k_1 = 12$). (a) Signal at (A, 20° , 0.24). The electrical control activity and its spectrum show a distinctly abnormal signal at 6.8 cycles/min. (b) Signal at (A, 120° , 0.24). The electrical control activity looks almost normal, but its spectrum shows strong peaks at 3 and 6.8 cycles/min. (c) Signal at (A, 160° , 0.24). Both the electrical control activity and its spectrum look normal.

This suggests the use of multichannel EGG recordings as discussed below.

The analysis of the simulated surface EGG was based on the strength of the normal component, p_n . The strongest signal peak, p_n , occurred in an anterior patch of the surface that is higher up on the left side of the median ($\theta > 180^\circ$) than on its right side ($\theta > 0^\circ$). This is consistent with the area of the surface considered optimum for recording surface EGG's [4]. When normal EGG's are recorded in a clinical setting with currently available methodology, one wants to know the probability that the patient is truly healthy and that an abnormality present in the stomach was not diagnosed from the recorded EGG. Obviously, in the diseased state, the recorded signal should not be normal. Therefore, p_n should ideally be zero, or at the very least, a relatively small number. The pitfalls in the predictive value of this method are implicit in the fact that Table I and Fig. 9(a)–(c) confirm that normal simulated EGG's may be recorded in the diseased state.

In the model, visual scoring of surface signals from "diseased sources" may reveal a normal or an abnormal waveform, depending on the electrode location and the percentage of "diseased" sources. Power spectrum analysis did not improve the situation. Fig. 9 shows simulated waveforms at different locations on the torso with 54.5% of the oscillating sources abnormal, i.e., $k_1 = 12$. The waveform and frequency spectrum at some locations on the surface strongly suggest tachygastric at 6.8 cycles/min (Fig. 9a). At other locations, the decision as to

normality of the signal could go either way (Fig. 9(b)), while one would unwittingly diagnose others as normal (Fig. 9(c)). These observations are consistent with what is seen in actual measurements, as depicted in Fig. 8(a) and (b). This explains the "normal" appearance of the cutaneous EGG shown in the postoperative recording in Fig. 8(a). The percutaneous and proximal antral activities appear normal at a fundamental frequency of 2.85 cycles/min. The frequency of the activity at the most distal serosal site, E3, at 4.23 cycles/min is roughly 1.5 times that of the signals on the more proximal serosal electrodes, E1 and E2 and the cutaneous electrode, E0. Therefore, if one employs multiple channels and dissimilar frequencies appear on the different channels, frequency-uncoupled gastric electrical abnormality is a likely diagnosis.

Bearing in mind anatomical variability, the region on the model at which the strongest normal signal peaks were detected corresponds approximately to a region described by parallel horizontal lines through the umbilicus and the sternal apex, and vertical lines extending downwards from the nipples (Figs. 2(a) and 3(a)). Visual scoring of the signals recorded in this region in man confirms normal EGG 67% of the time; this percentage becomes 95 if spectral analysis is employed. These observations are consistent with the simulation results. They support the assertion that GEA in health can be detected with respectable accuracy using the cutaneous method. The same is not true when frequency and phase abnormalities were introduced into the simulation.

Finally, the main objective of this study is to present a mathematical model of the surface EGG in disease. The authors are not aware of any existing models. The main strength of the model is its ability to simulate different kinds of gastric electrical abnormalities. The model represented by (1) and (2) is a simplified model of the actual system. The actual control of gastric motility involves an integration of myogenic, nervous, and hormonal factors. One might ask if a more mathematically involved model will not be a better approximation. The accuracy of any model generally improves as one incorporates more properties of the actual system. For instance, one could incorporate changes in the shape and location of the antrum into the model by making the source locations variable. This will represent situations in which the stomach is displaced by meals or lateral motion. The price for the increased accuracy is complexity and an exponential increase in the machine-hours required for computation. Therefore, judicious approximations to the real system are inevitable. In the model presented here, simplifying assumptions have been undertaken to reduce computational tedium. However, we believe that this model is adequate for the purposes intended. Comparison of the results of this simulation and actual human studies may be employed as a measure of its validity.

The important consideration for clinical electrogastrography is the predictive value of the method in diagnosing abnormalities. In its present configuration, the method employs mainly the frequency and amplitude of the surface EGG as diagnostic parameters. The frequency spectrum of the EGG at any single location on the surface performs poorly in the diagnosis of abnormalities involving uncoupled GEA. One way around this problem is to measure the EGG at several locations and

develop an algorithm for evaluating these composite records. A better way is to develop a standard electrode array that improves the diagnostic accuracy. Simulation of EGG's in health and disease over the entire anterior surface similar to that presented in this study may be used to develop such an electrode configuration that will diagnose abnormalities with better accuracy. Empirical methods may then be employed to validate such results. On the other hand, the amplitude of the cutaneous signal may be useful in determining the velocity of propagation of the antral signal, if the displacement element can be factored out.

APPENDIX

The potential ϕ due to a current source of strength I in a volume of conductivity σ can be described by Poisson's equation [37]

$$\nabla^2 \phi = -\frac{I}{\sigma} \quad (\text{A1})$$

subject to the boundary conditions:

- 1) ϕ is finite inside the volume, and
- 2) Neumann's boundary condition $\left[\frac{\partial \phi}{\partial n}\right]_s = 0$, (\underline{n} is the normal vector at the surface s).

The system of interest is synchronized with respect to time for all field quantities and quasi-static. This idea of the system being quasi-static plays an important role in simulation. Since transient effects can be ignored, it is easy to perform sampling in time and space. Sampling in time allows one to obtain the system solution at each sample instance and by superposition simulate the time dependency of the system. A solution of (A1) in infinite space is

$$\phi_\infty = \frac{I}{4\pi\sigma} \cdot \frac{1}{R} \quad (\text{A2})$$

where $R^2 = \rho^2 + (z - z_0)^2$ for $\rho^2 = r^2 + r_0^2 - 2r_0 \cos(\theta - \theta_0)$. Expanding $\frac{1}{R}$ so that the expression converges for $r > r_0$ gives

$$\frac{1}{R} = \frac{2}{\pi} \int_0^\infty \cos \xi(z - z_0) \cdot K_0(\xi\rho) d\xi \quad (\text{A3})$$

where

$$K_0(\xi\rho) = \sum_{m=0}^{\infty} \epsilon_m \cos m(\theta - \theta_0) \cdot I_m(\xi r_0) k_m(\xi r), \quad r > r_1$$

$$K_0(\xi\rho) = \sum_{m=0}^{\infty} \epsilon_m \cos m(\theta - \theta_0) \cdot I_m(\xi r) K_m(\xi r_0), \quad r < r_1$$

and

$$\begin{aligned} \epsilon_m &= 1, & m &= 0 \\ \epsilon_m &= 2, & m &\geq 1. \end{aligned}$$

l_m and k_m are the modified Bessel functions of order m of the first and second kind, respectively [38].

Hence, (A3) becomes

$$\begin{aligned} \phi_\infty &= \frac{1}{2D\pi^2\sigma} \int_0^\infty I \cdot \cos \xi(z - z_0) \\ &\cdot \sum_{m=0}^{\infty} I_m \cos m(\theta - \theta_0) \cdot I_m(\xi r_0) \cdot K_m(\xi r) d\xi. \quad (\text{A4}) \end{aligned}$$

If we now replace the current source by a single dipole (SD) of dipole moment \underline{P} , the equivalent of (A4) may be obtained by differentiating ϕ_m with respect to the direction of the dipole moment. The dipole moment may then be resolved into its r , θ , and z components as $\underline{P} = P(P_r, P_\theta, P_z)^T$.

The solution for a single current dipole of dipole moment $P(0, 0, P_z)^T$ is obtained by differentiating (A4) with respect to z and replacing I with $-P_z$. Therefore,

$$\begin{aligned} \frac{\delta \phi}{\delta r} &= \frac{\delta}{\delta r} \left[\frac{P_z}{2\pi^2\sigma} \int_0^\infty \xi \sin(z - z_0) \cdot c_1 \right. \\ &\cdot \sum_{m=0}^{\infty} \epsilon_m (K_m(\xi r) + c_2 I_m(\xi r)) \\ &\cdot I_m(\xi r_0) \cos m(\theta - \theta_0) \left. \right]_{r=A} d\xi = 0 \end{aligned}$$

where

$$\begin{aligned} c_1 &= f(h, \xi), \quad \text{and} \\ c_2 &= -\frac{\dot{K}_m(\xi A)}{\dot{I}_m(\xi A)}. \end{aligned}$$

The "dot" denotes differentiation with respect to the argument. By imposing the other boundary condition $\left[\frac{\delta \phi}{\delta z}\right]_{z=0,h} = 0$, c_1 is evaluated to be a periodic impulse function of strength $\frac{2\pi}{h}$ at $\xi = \frac{n\pi}{h}$, $n = 0, 1, 2, \dots$. Therefore,

$$\begin{aligned} \phi_z|_{r=A} &= \frac{-2P_z}{\pi Ah\sigma} \cdot \sum_{n=0}^{\infty} \sin \frac{n\pi z_0}{h} \cos \frac{n\pi z}{h} \\ &\cdot \sum_{m=0}^{\infty} \epsilon_m \left\{ \frac{I_m\left(\frac{n\pi r_0}{h}\right) \cos(\theta - \theta_0)}{I_{m-1}\left(\frac{n\pi A}{h}\right) + I_{m+1}\left(\frac{n\pi A}{h}\right)} \right\}. \quad (\text{A5}) \end{aligned}$$

Equation (A5) is what one needs to evaluate ϕ_z at the time and space sample points chosen for the z component of the SD. In a similar manner, solutions can be obtained for ϕ_r and ϕ_θ

$$\begin{aligned} \phi_r &= \frac{-2P_r}{\pi Ah\sigma} \cdot \sum_{n=0}^{\infty} \cos \frac{n\pi z_0}{h} \cos \frac{n\pi z}{h} \cdot \sum_{m=0}^{\infty} 1/2\epsilon_m \\ &\times \left\{ \frac{I_{m-1}\left(\frac{n\pi r_0}{h}\right) + I_{m+1}\left(\frac{n\pi r_0}{h}\right)}{I_{m-1}\left(\frac{n\pi A}{h}\right) + I_{m+1}\left(\frac{n\pi A}{h}\right)} \right\} \cos(\theta - \theta_0) \quad (\text{A6}) \end{aligned}$$

and

$$\begin{aligned} \phi_\theta &= \frac{2P_\theta}{\pi Ah\sigma} \cdot \sum_{n=0}^{\infty} \cos \frac{n\pi z_0}{h} \cos \frac{n\pi z}{h} \cdot \sum_{m=0}^{\infty} 1/2\epsilon_m \\ &\times \left\{ \frac{I_{m-1}\left(\frac{n\pi r_0}{h}\right) + I_{m+1}\left(\frac{n\pi r_0}{h}\right)}{I_{m-1}\left(\frac{n\pi A}{h}\right) + I_{m+1}\left(\frac{n\pi A}{h}\right)} \right\} \sin(\theta - \theta_0). \quad (\text{A7}) \end{aligned}$$

REFERENCES

- [1] C. F. Code, J. H. Szurszewski, K. A. Kelly, and I. B. Smith, "A concept of control of gastrointestinal motility," in *Handbook of Physiology: Alimentary Canal*, C. F. Code, Ed. 1968, sec. 6, vol. 5.
- [2] E. E. Daniel and K. M. Chapman, "Electrical activity of the gastrointestinal tract as an indication of mechanical activity," *Amer. J. Dig. Dis.*, vol. 85, p. 54, 1963.
- [3] T. Y. El-Sharkawy, K. G. Morgan, and J. H. Szurszewski, "Intracellular electrical activity of canine and human gastric smooth muscle," *J. Physiol. (London)*, vol. 279, pp. 291-307, 1978.

- [4] N. Mirrizi and U. Scafoglieri, "Optimal direction of the electrogastric signal in man," *Med. Biol. Eng. Comput.*, vol. 21, pp. 385-389, 1983.
- [5] J. W. Hamilton, B. E. Bellahsene, M. Reichelder, J. G. Webster, and P. Baas, "Human electrogastragrams: Comparison of surface and mucosal recordings," *Dig. Dis. Sci.*, vol. 31, pp. 33-39, 1986.
- [6] T. L. Abell and J.-R. Malagelada, "Glucagon evoked gastric dysrhythmias in humans shown by an improved electrogastrographic technique," *Gastroenterol.*, vol. 88, no. 6, pp. 1932-1940, 1985.
- [7] B. E. Bellahsene, J. W. Hamilton, J. G. Webster, P. Bass, and M. Reichfelder, "An improved method for recording and analyzing the electrical activity of the human stomach," *IEEE Trans. Biomed. Eng.*, vol. BME-32, no. 11, pp. 911-915, 1985.
- [8] B. O. Familoni, Y. J. Kingma, and K. L. Bowes, "A study of transcutaneous and intraluminal measurements of gastric electrical activity in humans," *Med. Biol. Eng. Comput.*, vol. 25, pp. 397-402, 1987.
- [9] R. M. Stern, K. L. Koch, W. R. Stewart, and M. W. Vasey, "Electrogastrography: Current issues in validation and methodology," *Psychophysiol.*, vol. 24, no. 1, pp. 55-64, 1987.
- [10] H. Geldof, E. J. Van Der Schee, M. Van Blankenstein, and J. L. Grashuis, "Electrogastrographic study of gastric myoelectrical activity in patients with unexplained nausea and vomiting," *GUT*, vol. 27, pp. 799-808, 1986.
- [11] C. H. You, K. Y. Lee, W. Y. Chey, and R. Mengur, "Electrogastrographic study of patients with unexplained nausea, bloating and vomiting," *Gastroenterol.*, vol. 79, pp. 311-314, 1980.
- [12] T. L. Abell *et al.*, "Gastric electromechanical and neurohormonal function in anorexia nervosa," *Gastroenterol.*, vol. 93, pp. 958-965, 1987.
- [13] T. L. Abell, M. Camilleri, and J.-R. Malagelada, "High prevalence of gastric electrical dysrhythmias in diabetic gastroparesis," *Gastroenterol.*, vol. 88, p. 1299, 1985.
- [14] C. J. Pfister, J. W. Hamilton, N. Nagel, P. Bass, J. G. Webster, and W. Tompkins, "Use of spectral analysis in the detection of frequency differences in the electrogastragrams of normal and diabetic subjects," *IEEE Trans. Biomed. Eng.*, vol. 35, no. 11, pp. 935-941, 1988.
- [15] K. L. Koch, R. M. Stern, M. Vasey, J. J. Botti, G. W. Creasey, and A. Dwey, "Gastric dysrhythmia and nausea of pregnancy," *Dig. Dis. Sci.*, vol. 35, no. 8, pp. 961-968, 1990.
- [16] R. M. Stern, K. L. Koch, H. W. Liebowitz, I. M. Lindblad, C. L. Shupert, and W. R. Stewart, "Tachygastria and motion sickness," *Aviat. Space Environ. Med.*, vol. 56, pp. 1074-1077, 1985.
- [17] B. O. Familoni, K. L. Bowes, Y. J. Kingma, and K. R. Cote, "Can transcutaneous recordings detect gastric electrical abnormalities?" *GUT*, vol. 32, no. 2, pp. 141-146, 1991.
- [18] M. P. Mintchev, Y. J. Kingma, and K. L. Bowes, "Accuracy of cutaneous recordings of gastric electrical activity," *Gastroenterol.*, vol. 104, pp. 1273-1280, 1993.
- [19] B. O. Familoni, Y. J. Kingma, and K. L. Bowes, "Noninvasive assessment of human gastric motor function," *IEEE Trans. Biomed. Eng.*, vol. BME-34, no. 1, pp. 30-36, 1987.
- [20] N. Mirrizi, R. Stella, and U. Scafoglieri, "A model of extracellular waveshapes of gastric electrical activity," *Med. Biol. Eng. Comput.*, vol. 23, pp. 33-37, 1985.
- [21] ———, "Model to simulate the gastric electrical control and response activity on the abdominal wall and on the abdominal surface," *Med. Biol. Eng. Comput.*, vol. 24, pp. 157-163, 1986.
- [22] S. K. Sarna, E. E. Daniel, and Y. J. Kingma, "Simulation of the electric activity of the stomach by an array of relaxation oscillators," *Dig. Dis.*, vol. 17, pp. 299-310, 1972.
- [23] S. K. Sarna, "Computer models of gastrointestinal electrical control activity," Ph.D. dissertation, Univ. of Alberta, Edmonton, 1972.
- [24] R. Plonsey, *The Bioelectric Phenomena*. New York: McGraw-Hill, 1979, pp. 202-209.
- [25] O. B. Wilson, J. W. Clark, N. Ganapathy, and T. L. Harman, "Potential field from an active nerve in an inhomogeneous, anisotropic volume conductor—The forward problem," *IEEE Trans. Biomed. Eng.*, vol. BME-32, no. 12, pp. 1032-1041, 1985.
- [26] W. T. Miller and D. B. Geselowitz, "Simulation studies of the electrocardiogram I. The normal heart," *Circ. Res.*, vol. 43, pp. 301-315, 1978.
- [27] R. M. Stern and K. L. Koch, Eds., *Electrogastrography*. New York: Praeger, 1985.
- [28] T. S. Nelsen and S. Kohatsu, "Clinical electrogastrography and its relationship to gastric surgery," *Amer. J. Surg.*, vol. 116, pp. 215-222, 1968.
- [29] S. K. Sarna, K. L. Bowes, and E. E. Daniel, "Post-operative gastric electrical control activity in man," in *Gastrointestinal Motility*, E. E. Daniel, Ed. Vancouver: Mitchell, 1974.
- [30] J. A. McIntyre, M. Deitel, M. Baida, and S. Jalil, "The human electrogastragram at operation: A preliminary report," *Canadian J. Surg.*, vol. 12, pp. 275-284, 1969.
- [31] B. O. Familoni, T. L. Abell, and G. Voeller, "Measurement of gastric and small bowel electrical activity at laparoscopy," *J. Laparoendoscopic Surg.*, vol. 4, no. 5, pp. 325-332, 1994.
- [32] A. J. P. M. Smout, E. J. van der Schee, and J. L. Grashuis, "What is measured in electrogastrography?" *Dig. Dis. Sci.*, vol. 25, pp. 179-187, 1980.
- [33] ———, "Postprandial and interdigestive gastric electrical activity in the dog recorded by means of cutaneous electrodes," in *Gastrointestinal Motility*, J. Christensen, Ed. New York: Raven, 1980, pp. 187-194.
- [34] J. Chen and R. W. McCallum, "Response of the electric activity in the human stomach to water and a solid meal," *Med. Biol. Eng. Comput.*, vol. 29, pp. 351-357, 1991.
- [35] J. W. Hamilton, B. E. Bellahsene, M. Reichelder, J. G. Webster, and P. Baas, "Human electrogastragrams: Comparison of surface and mucosal recordings," *Dig. Dis. Sci.*, vol. 31, pp. 33-39, 1986.
- [36] R. M. Stern, H. E. Crawford, W. R. Stewart, M. W. Vasey, and K. L. Koch, "Sham feeding: Cephalic-vagal influences on gastric myoelectric activity," *Dig. Dis. Sci.*, vol. 34, pp. 521-527, 1989.
- [37] P. M. Morse and M. Feshback, *Methods of Theoretical Physics*. New York: McGraw-Hill, 1953.
- [38] R. H. Okada, "Potentials produced by an eccentric dipole in a circular finite length conducting cylinder," *IRE Trans. Med. Electron.*, vol. ME-7, p. 14, 1956.



Babajide O. Familoni was born in Nigeria where he received the B.Sc. degree in electrical engineering at the University of Lagos in 1978. He received the Ph.D. in electrical engineering from the University of Alberta, Edmonton, Canada in 1986.

He is currently an Associate Professor at the University of Memphis and an Adjunct Assistant Professor of Biomedical Engineering at the University of Tennessee-Memphis. His areas of interest include intelligent control systems and gut electrophysiology and motor function.



Thomas L. Abell obtained medical degrees at Yale University (B.A., 1971) and the University of South Dakota (B.S.M., 1975 and M.D., 1977). He served residency at Southern Illinois University (1977-78), Ohio State University (1978-80), and the University of Tennessee-Memphis (1986-87). He completed fellowships at the Mayo Clinic (1982-86) and the University of Tennessee-Memphis (1987-88).

He is currently an Associate Professor and Director of the Gastroenterology Motility Laboratory in the Division of Gastroenterology, Department of Medicine at the University of Tennessee-Memphis. His areas of interest include clinical and research gastrointestinal electrophysiology and motility disorders, fecal incontinence, chronic constipation, diabetic enteropathy, pancreas/kidney transplantation, and autonomic function testing.

Kenneth L. Bowes was born in Imperial, Saskatchewan, Canada. He received the M.D. degree from Queen's University, Kingston, Ontario, Canada in 1962, the M.Sc. degree in experimental surgery from the University of Alberta in 1965, and a fellowship from the Canadian Royal College of Surgeons in 1967.

Since 1971, he has worked in the Department of Surgery at the University of Alberta Hospital, Edmonton, Alberta, Canada. He is currently Professor of Surgery in that Department.

Dr. Bowes was a Medical Research Council of Canada Fellow in 1968 and 1969, and a McLaughlin Foundation Research Fellow in 1969 and 1970.